IEEE Access
Multidisciplinary | Rapid Review | Open Access Journal

Received October 19, 2017, accepted December 4, 2017, date of publication December 18, 2017,
date of current version February 14, 2018.

Digital Object Identifier 10.1109/ACCESS.2017.2784846

Low-Voltage Ride-Through Control Strategy for a Virtual Synchronous Generator Based on Smooth Switching

KAI SHI[1], WENTAO SONG[1], PEIFENG XU[1], RONGKE LIU[2], ZHIMING FANG[1], AND YI JI[1]
[1]School of Electrical and Information Engineering, Jiangsu University, Zhenjiang 212000, China
[2]KTK Group, Changzhou 213102, China

Corresponding author: Peifeng Xu (xupeifeng2003@126.com)

This work was supported in part by the National Natural Science Foundation of China under Grant 51407085, in part by the China Postdoctoral Science Foundation Funded Project under Grant 2015M571685, in part by the Project Funded by the Priority Academic Program Development of Jiangsu Higher Education Institution, and in part by the Jiangsu University Senior Talents Special Project under Award 13JDG111.

ABSTRACT The grid-connected inverter with virtual synchronous generator (VSG) control technology can improve the friendliness of a distributed power supply to the power grid. However, its low-voltage ride-through (LVRT) capability is insufficient, which results in difficulties in limiting the current and provide reactive power support. A new LVRT control strategy based on the smooth switching is proposed in this paper. In this strategy, the voltage source mode of VSG is transformed into current source mode to limit the output current and provide reactive power support through the proportional resonance current control algorithm under grid fault. Furthermore, the feedback tracking synchronization strategy of the phase angle is employed to realize the smooth switching between two modes. When the grid fault recovers, it can directly switch back to grid-connected operation mode through a delay module without an additional algorithm. The simulation results verify the correctness and feasibility of the proposed control strategy.

INDEX TERMS Grid fault, low-voltage ride through, smooth switching, VSG.

I. INTRODUCTION

As the global energy crisis and environmental problems become increasingly serious, the development of distributed power supplies has attracted much attention [1], [2]. Because of the high exploitation and utilization permeability of new energy resources and a large number of new grid-connected loads, the trend of power electronics in the traditional power grid is gradually accelerating, and the alienation behaviour characteristics of the power system has become increasingly obvious [3]–[6].

In recent years, scholars have focused on the grid-connected inverter based on the virtual synchronous generator (VSG) [7]–[9]. The basic idea is to simulate the characteristics of the synchronous generator (SG) and provide inertial and damping support to the grid [10], [11]. A mathematical model of an inverter based on VSG control was established, and the active and reactive power control strategy of the VSG was designed in [12] and [13]. The pre-synchronization control strategy and parallel operation of VSG were proposed in [14]–[17]; this approach improves the operation performance of the VSG. A constant power control method of VSG was proposed in [18] to output a constant active and reactive power to the grid when the amplitude and frequency of the grid voltage change. The stability of a grid-connected VSG was analysed, and a parameter optimization method was proposed in [19].

However, the research on VSG technology is primarily based on normal grid operation, and the distribution network is susceptible to short circuit faults in actual operation. Thus, the grid-connected inverter requires LVRT capability, i.e., limiting the amplitude of the grid current and providing reactive power support for the grid under grid fault [20]. The current VSG technology cannot easily provide reactive power support and can even damage electrical equipment via a high output current. The research on the LVRT of the traditional grid-connected inverter is relatively mature and possesses a good reference value. In [21]–[23], the setting methods of the current and power reference value under different control

strategies were studied with the aim of controlling the current peak. The current loop was employed in [24] to enhance the inertia of VSG and the ability of LVRT through the power angle. However, the parameters were too extreme for engineering application. A relatively complete LVRT control scheme was proposed in [25], including the method of fault detection, the design of active and reactive current instruction, and the control logic processing.

The above control strategies or algorithms are all complicated and have a variety of parameters. Moreover, some of these strategies are only verified preliminarily, without the integrity test under grid fault; thus, they do not satisfy the engineering requirements. In this paper, a smooth switching based on the VSG control algorithm and the PR current control algorithm is proposed to realize the LVRT and simplify the control method. A feedback tracking synchronization strategy of the phase angle is adopted to realize smooth switching. The proposed new method can not only accelerate the transient process under grid fault but also limit the output current and provide reactive power support. Therefore, both the operation of the VSG under grid fault and the improvement of the transient performances are realized.

II. BASIC PRINCIPLE

A. BASIC PRINCIPLE OF VSG TECHNOLOGY

The main circuit of VSG and the control block diagram is shown in Fig. 1, in which the inverter bridge circuit is formed with power device Q_1-Q_6 and inverter side inductance L_1, filter capacitor C and grid side inductance L_2 commonly constitute the LCL filter. As the main circuit of the grid-connected inverter is equivalent to the electrical parts of SG, the fundamental wave of the grid-connected inverter bridge arm midpoint e_a, e_b, e_c is considered the inner electric potential of SG, the inverter side inductance L_1 is considered the synchronous reactance of SG, and the output inverter voltage v_{ao}, v_{bo}, v_{co} is considered the terminal voltage of SG [4].

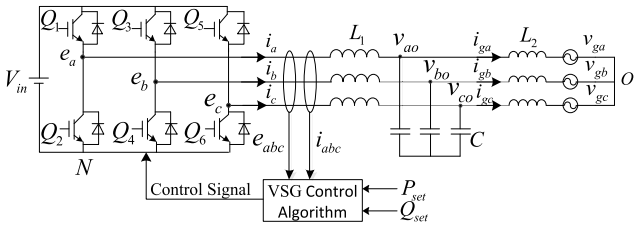

FIGURE 1. VSG main circuit and control structure.

The basic idea of the VSG algorithm is to simulate the operation characteristics of SG via active and reactive power loops. To provide a PWM modulated wave signal to grid-connected inverter, the active power loop outputs the frequency and phase of inverter modulated wave, and the reactive power loop outputs the amplitude of inverter modulated wave.

The specific mathematical model of the VSG control algorithm in Fig. 1 can be described as follows [7]:

$$\begin{cases} P_{set} + D_p(\omega_n - \omega) - P_e = J\omega_n \dfrac{d\omega}{dt} \\ Q_{set} + D_q(V_n - V) - Q_e = K\dfrac{dE_m}{dt} \\ \theta = \displaystyle\int \omega dt \end{cases} \tag{1}$$

where P_{set} and Q_{set} are the given active and reactive power, respectively, D_p and D_q are the droop coefficients of P-f and Q-V, respectively, P_e and Q_e are the actual output active and reactive power, respectively, J and K are the inertia coefficients of active and reactive power loops, respectively, ω_n and ω are the rated angular frequency and the actual rotor angular frequency, respectively, V_n and V are the effective value of rated voltage amplitude and the actual output voltage amplitude, respectively, E_m is the inner electric potential of VSG, and θ is the actual rotor position angle.

B. BASIC PRINCIPLE OF POSITIVE AND NEGATIVE SEQUENCE SEPARATION

Tracking the amplitude, frequency and phase of the grid voltage is indispensable for an inverter grid connection. Decoupled Double Synchronous Reference Frame PLL (DDSRF-PLL) is employed in this paper to separate the three-phase asymmetrical voltage into positive and negative sequence components and then track the frequency and phase of the positive sequence component through SRF-PLL. DDSRF-PLL completely decouples the positive and negative sequence components to eliminate the role of the negative sequence component without reducing the bandwidth [22].

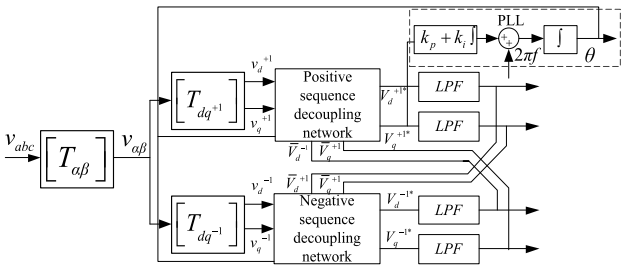

FIGURE 2. Block diagram of DDSRF-PLL.

The entire structure diagram of DDSRF-PLL is shown in Fig. 2. The voltage equation under the dq^{+1}, dq^{-1} coordinate system from the three-phase stationary coordinate system could be obtained through the Clark and Park transformation. It is clear that the DC component under the negative sequence reference coordinate system arouses the AC component under positive sequence reference coordinate system and vice versa; this behaviour is affected by the rotation transformation matrix of angular frequency 2ω. Thus, the feedback control is used to eliminate the coupling, by which the coupling operation caused by frequency oscillation 2ω under its own coordinate axis could be eliminated.

As a result, the three-phase asymmetrical voltage could be separated into positive and negative sequence components, and the phase could be locked through PLL.

In Fig. 2, v_{abc} and $v_{\alpha\beta}$ are the grid voltage amplitude under three-phase and two-phase stationary coordinate systems, respectively, $v_{dq}^{\pm 1}$ is the positive and negative sequence voltage under double synchronous reference coordinate, $V_{dq}^{\pm 1*}$ is the estimated value of the output voltage, $\overline{V}_{dq}^{\pm 1}$ is the feedback DC voltage component, $[T_{\alpha\beta}]$ is the matrix of the Clark transformation, $[T_{dq+1}]$ and $[T_{dq-1}]$ are the matrices of Park transformation under dq^{+1} and dq^{-1} coordinate systems, respectively, k_p and k_i are the PI coefficients of PLL, and the low-pass filter (LPF) is

$$LPF(s) = \frac{\omega_f}{s + \omega_f} \tag{2}$$

where ω_f is the cut-off frequency of the low-pass filter. Considering the balance between the oscillation suppression and the time response, the parameter ω_f is set as $\omega/\sqrt{2}$.

The specific arithmetic expression of the positive and negative sequence voltage components can be described as follows:

$$\begin{bmatrix} V_d^{+1*} \\ V_q^{+1*} \end{bmatrix} \approx \begin{bmatrix} v_d^{+1} \\ v_q^{+1} \end{bmatrix} - \bar{V}_d^{-1} \begin{bmatrix} \cos(2\theta) \\ -\sin(2\theta) \end{bmatrix} - \bar{V}_q^{-1} \begin{bmatrix} \sin(2\theta) \\ \cos(2\theta) \end{bmatrix} \tag{3}$$

$$\begin{bmatrix} V_d^{-1*} \\ V_q^{-1*} \end{bmatrix} = \begin{bmatrix} v_d^{-1} \\ v_q^{-1} \end{bmatrix} - \bar{V}_d^{+1} \begin{bmatrix} \cos(2\theta) \\ \sin(2\theta) \end{bmatrix} - \bar{V}_q^{+1} \begin{bmatrix} -\sin(2\theta) \\ \cos(2\theta) \end{bmatrix} \tag{4}$$

C. BASIC PRINCIPLE OF THE PROPORTIONAL RESONANCE (PR) CURRENT CONTROLLER

Double PI current regulators under the dq rotating coordinate system can meet the control requirement when the grid inverter works under normal conditions or disturbances, but they are not suitable for asymmetrical faults. Therefore, it is indispensable to possess a quick dynamic response to track the changes of voltage and frequency to improve the transient performance. A notch filter should be a competent solution for the decomposed positive and negative sequence current by the double PI regulator control strategy; however, the delay caused by the notch filter would affect the dynamical performance. It is well known that there are two fixed-frequency closed-loop poles in the transfer function of PR current controller that increases the gain at that frequency. Thus, it possesses a good frequency tracking characteristic [10].

With a PR current regulator introduced into the control strategy, the corresponding transfer function is given as follows:

$$U_{g\alpha\beta}^* = F_{PR}(s)(I_{g\alpha\beta}^* - I_{g\alpha\beta}) \tag{5}$$

where $U_{g\alpha\beta}^*$, $I_{g\alpha\beta}^*$, and $I_{g\alpha\beta}$ are the reference grid voltage, the reference grid current and the actual grid current, respectively, $F_{PR}(s)$ is the PR current regulator transfer function given by

$$F_{PR}(s) = K_p + R(s) = K_p + K_r \frac{s}{s^2 + \omega_1^2} \tag{6}$$

where K_p is the proportional coefficient used to adjust the dynamic performance of the system, K_r is the resonance coefficient, and ω_1 is the resonant angular frequency for the signal at the resonant frequency of the maximum gain to integrate.

The control block diagram is displayed in Fig. 3.

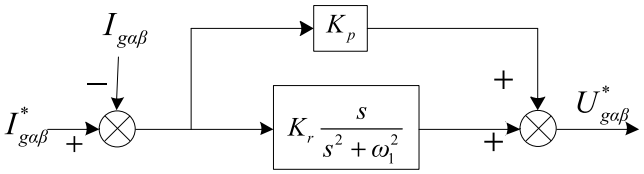

FIGURE 3. PR regulator control block diagram.

The Bode diagram of the resonant controller transfer function R(s) is shown in Fig. 4, where the resonance frequency of R(s) is ω_1.

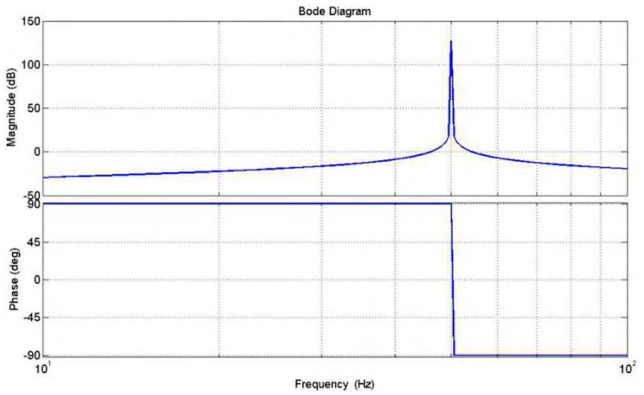

FIGURE 4. Bode diagram of the resonant controller.

Under the $\alpha\beta$ coordinate system, the positive and negative sequence components of the grid voltage and current rotate at the angular velocity of ω_1 and $-\omega_1$, respectively, when a grid voltage asymmetrical fault occurs. Therefore, a single resonant current regulator is employed to separately control the positive and negative sequence components of the inverter output current. According to the simulation results shown in the Bode diagram, the resonant regulator exclusively amplifies the current gain at the frequency of 50 Hz and suppresses the other frequency components. Thus, it is feasible for the employed single resonant current regulator to meet the control requirements.

III. ANALYSIS OF THE LVRT RESPONSE

To simplify the analysis process, we only discuss the operation under asymmetrical fault here. Considering the simplicity of the analysis, the LCL filter is replaced by L_g. Ignoring the line impedance and on-state resistance of the IGBT, the

equivalent circuit of the grid inverter under the three-phase static coordinate system is obtained as shown in Fig. 5, where $\boldsymbol{e_{abc}}$, $\boldsymbol{i_{abc}}$, L_g, and $\boldsymbol{v_g}$ are the three-phase inverter output voltage, three-phase inverter output current, filter inductance and three-phase grid voltage, respectively.

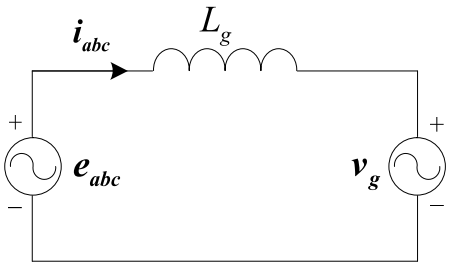

FIGURE 5. Equivalent circuit of the grid connected inverter under a static coordinate system.

When an asymmetrical fault occurs, the expression of the output complex power is [23]

$$\begin{aligned} S &= 1.5\boldsymbol{v_g}\boldsymbol{i}^*_{\boldsymbol{abc}} \\ &= 1.5(u^+_{dq}e^{j\omega t} + u^-_{dq}e^{-j\omega t})(i^+_{dq}e^{j\omega t} + i^-_{dq}e^{-j\omega t})^* \end{aligned} \tag{7}$$

where $\boldsymbol{i}^*_{\boldsymbol{abc}}$ denotes the conjugate complex number of the inverter output current, the subscripts d and q denote the components under two-phase rotational coordinates, and the superscripts $+$ and $-$ denote positive and negative sequence, respectively.

According to $S = P + \mathrm{j}Q$, the complex power is decomposed into active and reactive components. P and Q are given by

$$\begin{cases} P = P_0 + P_{c2}\cos(2\omega t) + P_{s2}\sin(2\omega t) \\ Q = Q_0 + Q_{c2}\cos(2\omega t) + Q_{s2}\sin(2\omega t) \end{cases} \tag{8}$$

where P_0 and Q_0 are the average values of P and Q; P_{c2} and P_{s2} are the double frequency fluctuation component amplitudes of P; and Q_{c2} and Q_{s2} are double frequency fluctuation component amplitudes of Q. These quantities are defined as follows:

$$\begin{cases} P_0 = \dfrac{3}{2}(u^+_d i^+_d + u^+_q i^+_q + u^-_d i^-_d + u^-_q i^-_q) \\ P_{c2} = \dfrac{3}{2}(u^-_d i^+_d + u^-_q i^+_q + u^+_d i^-_d + u^+_q i^-_q) \\ P_{s2} = \dfrac{3}{2}(u^-_q i^+_d - u^-_q i^+_q - u^+_q i^-_d + u^+_d i^-_q) \\ Q_0 = \dfrac{3}{2}(u^+_q i^+_d - u^+_d i^+_q + u^-_q i^-_d - u^-_d i^-_q) \\ Q_{c2} = \dfrac{3}{2}(u^-_q i^+_d - u^-_d i^+_q + u^+_q i^-_d - u^+_d i^-_q) \\ Q_{s2} = \dfrac{3}{2}(-u^-_d i^+_d - u^-_q i^+_q + u^+_q i^-_d + u^+_q i^-_q). \end{cases} \tag{9}$$

When an asymmetrical grid fault occurs, the decoupled dq-axis positive and negative sequence current components are used as controlled objects to realize the LVRT. From the mathematical relationship of (9), the control targets of VSG to achieve LVRT control under grid fault can be generalized into three types. The specific description of each type is given as follows:

1) TO OUTPUT SYMMETRICAL THREE-PHASE CURRENT

The solution to balance the three-phase current is mainly dependent on seeking a control strategy to eliminate the negative sequence component of current during the asymmetrical grid fault. To suppress the negative sequence component, we take $i^-_d = i^-_q = 0$ and do not attempt to eliminate the double frequency fluctuation components P_{c2}, P_{s2}, Q_{c2} and Q_{s2} here. Setting P_0 and Q_0 to the given value, the reference value of the positive and negative sequence current can be defined as follows:

$$\begin{cases} i^+_d = \dfrac{2}{3}\dfrac{P_0 u^+_d + Q_0 u^+_q}{(u^+_d)^2 + (u^+_q)^2} \\ i^+_q = \dfrac{2}{3}\dfrac{P_0 u^+_q - Q_0 u^+_d}{(u^+_d)^2 + (u^+_q)^2} \\ i^-_d = 0 \\ i^-_q = 0. \end{cases} \tag{10}$$

In target (1), the output current of the inverter is controlled as the three-phase symmetrical current, but both the active power and the reactive power contain double frequency fluctuation.

2) TO OUTPUT CONSTANT REACTIVE POWER

To provide reactive power support for the grid, outputting constant reactive power is indispensable for the system under asymmetrical grid fault. To suppress the double frequency fluctuation of reactive power, we take $Q_{c2} = Q_{s2} = 0$ and do not seek to eliminate P_{c2} and P_{s2}. Thus, the current reference value should be as follows:

$$\begin{cases} i^+_d = \dfrac{2}{3}\left(\dfrac{P_0 u^+_d}{D_2} + \dfrac{Q_0 u^+_q}{D_1}\right) \\ i^+_q = \dfrac{2}{3}\left(\dfrac{P_0 u^+_q}{D_2} - \dfrac{Q_0 u^+_d}{D_1}\right) \\ i^-_d = \dfrac{2}{3}\left(\dfrac{P_0 u^-_d}{D_2} - \dfrac{Q_0 u^-_q}{D_1}\right) \\ i^-_q = \dfrac{2}{3}\left(\dfrac{P_0 u^-_q}{D_2} + \dfrac{Q_0 u^-_d}{D_1}\right) \\ D_1 = (u^+_d)^2 + (u^+_q)^2 - (u^-_d)^2 - (u^-_q)^2 \\ D_2 = (u^+_d)^2 + (u^+_q)^2 + (u^-_d)^2 + (u^-_q)^2. \end{cases} \tag{11}$$

In target (2), the inverter output does not contain the reactive power of double frequency fluctuation, but contains the active power of double frequency fluctuation and three-phase asymmetrical current.

3) TO OUTPUT CONSTANT ACTIVE POWER

To suppress the active power of the double frequency fluctuation under grid fault, we choose the same solution as that used in target (2). We take $P_{c2} = P_{s2} = 0$, regardless

of Q_{c2} and Q_{s2}. The current reference value is described as follows:

$$\begin{cases} i_d^+ = \dfrac{2}{3}\left(\dfrac{P_0 u_d^+}{D_1} + \dfrac{Q_0 u_q^+}{D_2}\right) \\ i_q^+ = \dfrac{2}{3}\left(\dfrac{P_0 u_q^+}{D_1} - \dfrac{Q_0 u_d^+}{D_2}\right) \\ i_d^- = \dfrac{2}{3}\left(-\dfrac{P_0 u_d^-}{D_1} + \dfrac{Q_0 u_q^-}{D_2}\right) \\ i_q^- = \dfrac{2}{3}\left(-\dfrac{P_0 u_q^-}{D_1} - \dfrac{Q_0 u_d^-}{D_2}\right). \end{cases} \tag{12}$$

In target (3), the inverter output does not contain the active power of double frequency fluctuation but is involved in the reactive power of double frequency fluctuation and three-phase asymmetrical current.

IV. NEW CONTROL STRATEGY FOR LVRT

A. BASIC IDEA

According to the characteristics of the PR current controller, we propose a LVRT control strategy that switches from the VSG control mode to the PR current control mode when the grid fails and then returns to VSG control mode after the fault. The tentative control approach is shown in Fig. 6.

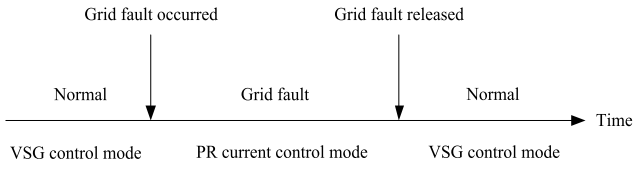

FIGURE 6. LVRT control schematic diagram of the VSG under grid fault.

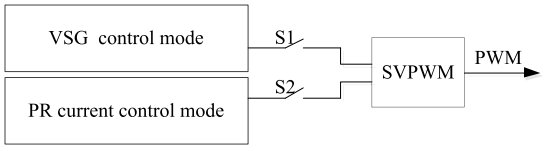

FIGURE 7. VSG low-voltage ride-through control block diagram.

The schematic block diagram of the proposed VSG LVRT control strategy is shown in Fig. 7. During normal operation, switch S1 is closed, and switch S2 is turned off. At the same time, the output of the PR current control mode must follow the grid voltage to ensure that the output variable value of two control algorithms is consistent. Once the grid fault occurs, the control algorithm immediately switches to the PR current control mode, with switch S2 closed and switch S1 open, to limit the grid current and provide reactive power to the grid. When the grid fault recovers, the control algorithm switches to the VSG control mode, with switch S1 closed and switch S2 open. The inverter system is continuously connected to the grid throughout the grid fault to ensure that it smoothly rides through the grid fault.

At the moment of switching from VSG control to PR current control, both of their output variables are voltages. However, the VSG control algorithm cannot track the grid voltage when the grid fails, resulting in the inequality of the variables and causing the controller output to vary during switching. In addition, even a small voltage deviation can lead to a large transient current shock because the VSG output impedance is very small and can damage the network or equipment. Thus, the specific control strategy should be employed to realize the smooth switching and achieve an excellent transient performance under grid fault.

B. MODE SWITCHING FROM NORMAL GRID-CONNECTED OPERATION TO GRID FAULT OPERATION

To guarantee the smooth switching between two control modes, two key factors should be considered. One is to ensure the consistency with the output variable properties of two control algorithms; in this paper, both of their output variables are voltages that satisfy this condition. Another key factor of the proposed LVRT control strategy is to ensure the consistency of the output variable value under two control algorithms.

Because the signals to the modulation module of the two control algorithms are all voltages, the core of the switching control is to search for the consistency of the two output values during switching. The allowable switching difference of the voltage amplitude, angular frequency and phase angle are respectively set to 15 V, 1.6 rad/s and 2×10^{-9}. The double-loop structure can quickly adjust the output voltage of the d, q-axis components to track the grid voltage vector. However, the phase angle lags through the PR controller, so the difficulty of switching control is ensuring the consistency of the phase angle under two control algorithms.

Equation (13) describes the relevant voltages:

$$\begin{cases} u_1 = U_1 \sin(\omega_1 t + \theta_0) \\ u_2 = U_2 \sin(\omega_2 t + \theta_i) \end{cases} \tag{13}$$

where u_1 and u_2 are the grid voltage vector and the output voltage vector, respectively, of the PR controller. Because $U_1 = U_2 = U$, the instantaneous difference between the voltages is described as

$$\begin{aligned} u_1 - u_2 &= U_1 \sin(\omega_1 + \theta_0) - U_2 \sin(\omega_2 + \theta_i) \\ &= 2U \sin\left(\frac{\omega_1 - \omega_2}{2} + \frac{\theta_0 - \theta_i}{2}\right) \\ &\quad \times \cos\left(\frac{\omega_1 + \omega_2}{2} + \frac{\theta_0 + \theta_i}{2}\right). \end{aligned} \tag{14}$$

A large amount of impact current may be produced when the voltages are not synchronized in the two control modes. If the rotation speed of u_2 is adjusted to make the two voltage vectors u_1 and u_2 coincide with each other, then the voltage synchronization and the smooth switching between the VSG control mode and the PR current control mode is realized. Thus, the feedback tracking synchronization strategy of the phase angle is designed as follows,

To synchronize the phase angle of the grid voltage vector and the output voltage vector of the PR controller, the phase angle of the grid voltage vector θ_0 obtained by the PLL is used as the phase angle value tracked by the controller

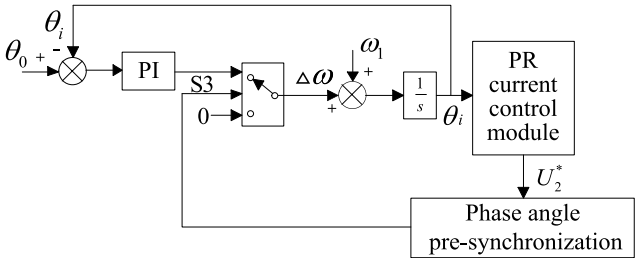

FIGURE 8. Feedback tracking synchronization diagram of the phase angle.

shown in Fig. 8. During the pre-synchronization of the phase angle, the modulation wave signal U_2^* informs the selection signal S3 to make differences between θ_0 and θ_i, and the phase angles are tracked through the PI regulator and negative feedback. In addition, at the moment the grid fault occurs, the phase angle of the PR controller is synchronized and remains at the normal grid value, which meets the requirements of smooth switching, so the control algorithm can directly switch from the VSG control mode to the PR current control mode.

C. MODE SWITCHING FROM GRID FAULT OPERATION TO NORMAL GRID-CONNECTED OPERATION

At the moment of grid fault recovery, a key question is determining how to switch back smoothly from the PR current control mode to the VSG control mode. At that time, it is too slow to use the VSG pre-synchronization control algorithm again to track of the grid voltage. Thus, the system still must operate in PR current control mode. Until grid fault recoveries, system switches back to the VSG control mode after few periods of delay.

D. ENTIRE CONTROL STRATEGY OF LVRT CONTROL

As shown in Fig. 9, when the grid operated in a normal state, the system is running in the VSG control mode, simulating the advantage of SG. When the grid fails, the system is switched to operate in the PR current control mode, suppressing the impact current and providing the reactive power support. The grid voltage is decoupled into U_d^+, U_q^+, U_d^-, and U_q^- by DDSRF-PLL, and the reference current is obtained via the mathematical relationship among current, power and voltage.

The PR current control mode is also running during the VSG control mode to enable the phase of output voltage to track that of the inverter output voltage. When a grid fault occurs, the system switches to the PR current control immediately, which involves disconnecting switch S_1 and closing switch S_2, to realize the LVRT. During the operating process of the PR current control, the frequency and amplitude of the output voltage in the VSG control mode are maintained. After the grid recovers to normal operation, the system can be switched directly back to the VSG control mode after a few seconds delay, which involves closing switch S_1 and disconnecting switch S_2.

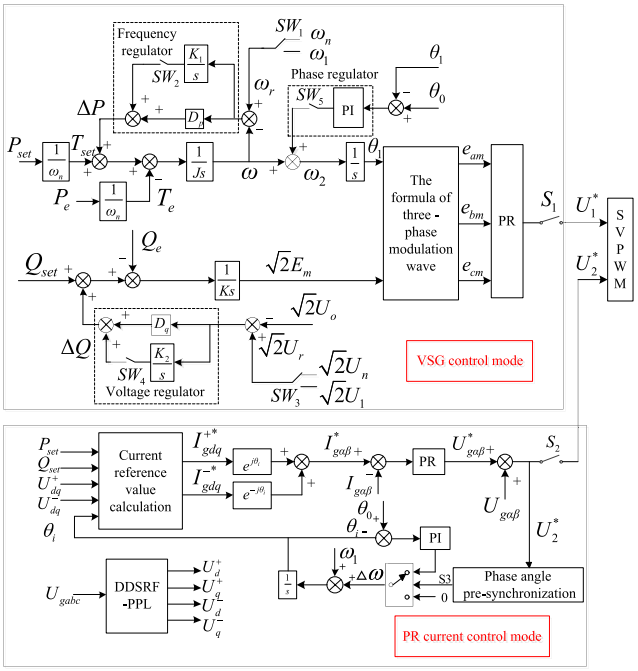

FIGURE 9. The entire control strategy of the LVRT system under grid fault.

TABLE 1. Specific simulation parameters.

Symbol	Quantity
V_{in}	600 V
e_{abc}	311 V
LCL	0.1 Ω, 3.2 mH
	2 Ω, 10 μF
	0.01 Ω, 0.8 mH
D_P	1590 W·s/rad
J	0.058 kg·m^2
D_q	320 A
K	6.5 A·s
P_{set}（Normal）	5 kW
Q_{set}（Normal）	450 Var
Switching Frequency	10 kHz
P（fault）	4 kW
Q（fault）	3 kVar

V. SIMULATION ANALYSIS AND VERIFICATION OF THE LVRT CONTROL STRATEGY

A. SIMULATION ANALYSIS OF THE VSG

The simulation model of the VSG under symmetrical grid fault is established in Matlab/Simulink. The specific simulation parameters are shown in Table 1, and the comprehensive simulation results are given below.

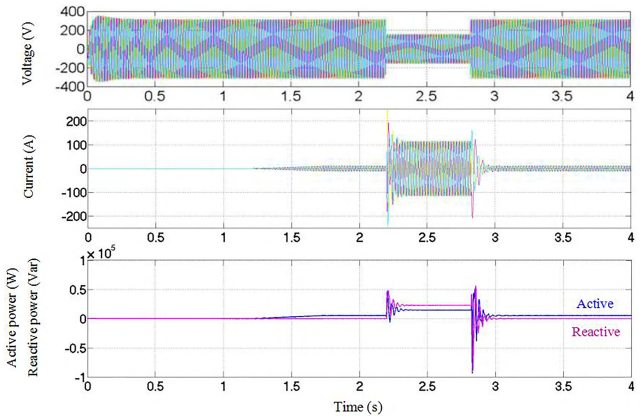

FIGURE 10. Simulation results of the VSG control strategy under symmetrical grid voltage fault.

As shown in Fig. 10, the grid voltage drops to 0.5pu at 2.2 s within 0.625 s, and the system runs in the VSG control mode. It can be seen that there is almost 250 A of impact current, both at 2.2 s and 2.825 s. During the grid fault, the active power and the reactive power fluctuate greatly in the case of a 50% grid voltage drop. It is predicted that the fluctuation range is more serious under a deeper drop. Thus, adopting the VSG algorithm alone is unable to realize LVRT.

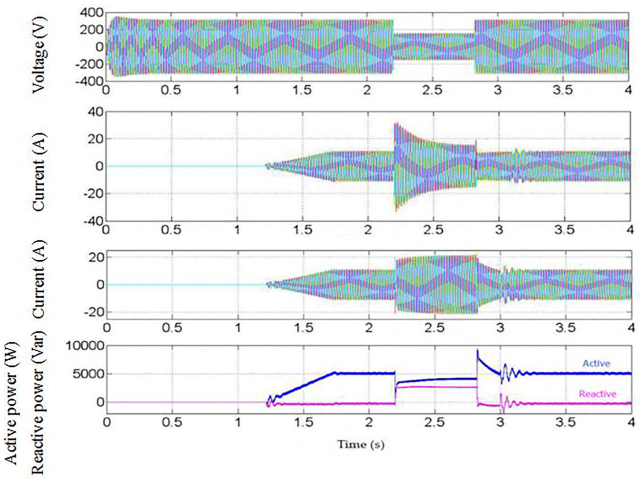

FIGURE 11. Simulation results of the LVRT control strategy under symmetrical grid voltage fault.

B. SIMULATION VERIFICATION OF LVRT

As shown in Fig. 11, the grid voltage drops to 0.5pu at 2.2 s within 0.625 s. The system is simulated both in the VSG control mode and the switching control mode with and without a feedback tracking synchronization strategy of the phase angle.

Comparing the simulation results under the two control strategies, the fault current under the VSG control strategy is almost five times that under the LVRT control strategy and the active power and the reactive power under the VSG control strategy fluctuate more greatly when the grid fault occurs and recovers. Using the LVRT control strategy proposed in this paper, it can be seen from the simulation results that there is an obvious current impact at 2.2 s without feedback tracking. However, there is symmetrical current without impact when a feedback tracking synchronization module is employed. Moreover, the active and reactive powers are stable during the grid fault. After the VSG algorithm is switched back at 3 s, the current and the power both exhibit a slight oscillation, but the system is stable during the whole LVRT process. The simulation results guarantee the correctness and effectiveness of the LVRT control strategy and the feedback tracking synchronization strategy of the phase angle proposed in this paper.

C. SIMULATION VERIFICATION OF ASYMMETRICAL GRID FAULT

For the three control targets described above, the same simulation environment is selected to verify the control effect under asymmetrical grid fault. At 2.2 s, phase A drops to 0.5pu, and phases B and C drop to 0.8pu within 0.625 s.

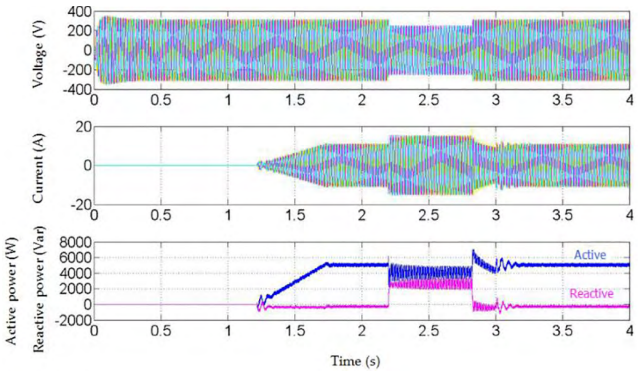

FIGURE 12. Simulation results with the target of symmetrical three-phase current under asymmetrical grid voltage fault.

The simulation results with the control target of outputting a symmetrical current are shown in Fig. 12. The current is symmetrical without impact at 2.2 s. However, the active power and the reactive power exhibit double frequency fluctuation, in agreement with the theoretical analysis. When the VSG algorithm is switched back at 3 s, the current and output power have a slight oscillation; however, there is no effect for the system to realize LVRT.

The simulation results with the control target of outputting stable active power are shown in Fig. 13. It can be seen that there is also no impact current at the initial stage of grid fault. During the fault, the active power is stable. However, the current contains the negative sequence component, and the reactive power exhibits double frequency fluctuation, in agreement with the theoretical analysis. After the fault, the VSG algorithm is switched back at 3 s, and the current and the power exhibit a slight oscillation that is the same as that of the previous case.

The simulation results with the control target of stable reactive power are shown in Fig. 14. During the fault,

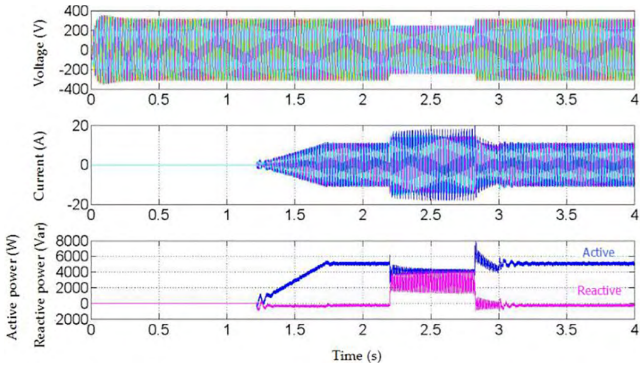

FIGURE 13. Simulation results with the target of stable active power under asymmetrical grid voltage fault.

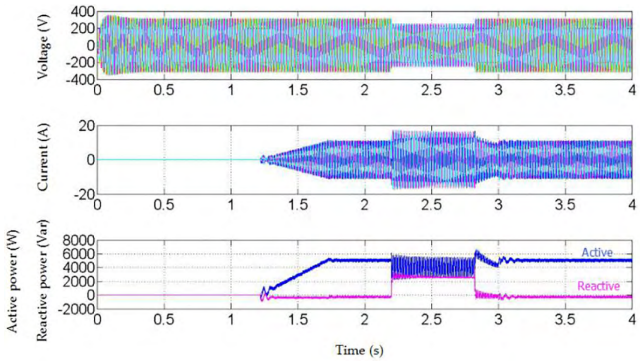

FIGURE 14. Simulation results with the target of stable reactive power under asymmetrical grid voltage fault.

the reactive power is stable. However, the current contains the negative sequence component without impact, and the output active power exhibits double frequency fluctuation, in agreement with the theoretical analysis. After the VSG algorithm is switched back at 3 s, the current and the power still exhibit a slight oscillation.

VI. CONCLUSION

In this paper, a LVRT control strategy of grid-connected inverter based on the VSG algorithm was proposed; the strategy is realized by the smooth switching between the PR current controller algorithm and the VSG control algorithm under grid fault. At the time of grid fault, the PR current control algorithm is used to limit the grid current and provides reactive power to the grid. A feedback tracking synchronization strategy of phase angle is employed to improve the transient performance during the switching process while reducing the complexity of switching control after grid fault recoveries. The detailed and complete simulation verification not only proves the effectiveness of the LVRT control strategy but also completely validates the operation performance with different control targets under asymmetrical voltage drop.

REFERENCES

[1] F. Gao and M. R. Iravani, "A control strategy for a distributed generation unit in grid-connected and autonomous modes of operation," *IEEE Trans. Power Del.*, vol. 23, no. 2, pp. 850–859, Apr. 2008.
[2] W. Du, Q. Jiang, and J. Chen, "Frequency control strategy of distributed generations based on virtual inertia in a microgrid," *Autom. Electr. Power Syst.*, vol. 35, no. 23, pp. 26–31, Dec. 2011.
[3] C.-S. Wang, Y. Li, and K. Peng, "Overview of typical control methods for grid-connected inverters of distributed generation," in *Proc. CSU-EPSA*, Jul. 2012, vol. 24. no. 2, pp. 12–20.
[4] L. Zhipeng *et al.*, "Virtual synchronous generator and its applications in micro-grid," in *Proc. CSEE*, Jun. 2014, vol. 34. no. 16, pp. 2591–2603.
[5] J. Zhang, L. Su, R. Liu, X. Zhang, and J. Su, "Small-signal stability analysis of grid-connected microgrid with inverter-interfaced distributed resources," *Autom. Electr. Power Syst.*, vol. 35, no. 6, pp. 76–80, Mar. 2011.
[6] Y. Li, D. M. Vilathgamuwa, and P. C. Loh, "Design, analysis, and real-time testing of a controller for multibus microgrid system," *IEEE Trans. Power Electron.*, vol. 19, no. 5, pp. 1195–1204, Sep. 2004.
[7] H. Bevrani, T. Ise, and Y. Miura, "Virtual synchronous generators: A survey and new perspectives," *Int. J. Electr. Power Energy Syst.*, vol. 54, pp. 244–254, Jan. 2014.
[8] T. Loix, "Participation of inverter-connected distributed energy resources in grid voltage control," Ph.D. dissertation, Katholieke Univ. Leuven, Leuven, Belgium, 2011.
[9] Z. Lü, L. An, J. Wenqian, and X. Xinwei, "New circulation control method for micro-grid with multi-inverter micro-sources," *Distrib. Utilization*, vol. 27, no. 1, pp. 40–47, Jan. 2012.
[10] M. Jianhui *et al.*, "Control strategy and parameter analysis of distributed inverters based on VSG," *Trans. China Electrotech. Soc.*, vol. 29, no. 12, pp. 1–11, Dec. 2014.
[11] M. Jianhui *et al.*, "Control strategy of DER inverter for improving frequency stability of microgrid," *Trans. China Electrotech. Soc.*, vol. 30, no. 4, pp. 70–79, Feb. 2015.
[12] Q.-C. Zhong and G. Weiss, "Static synchronous generators for distributed generation and renewable energy," in *Proc. Power Syst. Conf. Expo. (PSCE)*, Seattle, WA, USA, Apr. 2009, pp. 1–6.
[13] Q.-C. Zhong and G. Weiss, "Synchronverters: Inverters that mimic synchronous generators," *IEEE Trans. Ind. Electron.*, vol. 58, no. 4, pp. 1259–1267, Apr. 2010.
[14] Y. Liang and W. Cong, "The method of pre-synchronized grid-connection of synchronverter," *Power Syst. Technol.*, vol. 38, no. 11, pp. 3103–3108, Nov. 2014.
[15] S. Rongliang *et al.*, "Seamless switching control strategy for microgrid operation modes based on virtual synchronous generator," *Autom. Electr. Power Syst.*, vol. 40, no. 10, pp. 16–23, May 2016.
[16] M. Torres and L. A. C. Lopes, "Virtual synchronous generator: A control strategy to improve dynamic frequency control in autonomous power systems," *Energy Power Eng.*, vol. 5, no. 2, pp. 32–38, Apr. 2013.
[17] Y. Xiangwu *et al.*, "Small-signal stability analysis of parallel inverters with synchronous generator characteristics," *Power Syst. Technol.*, vol. 40, no. 3, pp. 910–917, Mar. 2016.
[18] Q.-C. Zhong, P.-L. Nguyen, Z. Ma, and W. Sheng, "Self-synchronized synchronverters: Inverters without a dedicated synchronization unit," *IEEE Trans. Power Electron.*, vol. 29, no. 2, pp. 617–630, Feb. 2014.
[19] Y. Du, J. Su, L. Chang, and M. Mao, "A mode adaptive frequency controller for microgrid," in *Proc. CSEE*, vol. 33, no. 19, pp. 67–75, Jul. 2013.
[20] *Technical Requirements for Connecting Photovoltaic Power Station to Power System*, document GB/T 19964-2012, China Electricity Council, Beijing, China, 2012.
[21] J. Miret, M. Castilla, A. Camacho, L. G. de Vicuña, and J. Matas, "Control scheme for photovoltaic three-phase inverters to minimize peak currents during unbalanced grid-voltage sags," *IEEE Trans. Power Electron.*, vol. 27, no. 10, pp. 4262–4271, Oct. 2012.
[22] A. Camacho, M. Castilla, J. Miret, A. Borrell, and L. G. de Vicuña, "Active and reactive power strategies with peak current limitation for distributed generation inverters during unbalanced grid faults," *IEEE Trans. Ind. Electron.*, vol. 62, no. 3, pp. 1515–1525, Mar. 2015.
[23] Q. Tan, Y. Xu, and H. Huang, "A control strategy for peak output current of PV inverter under unbalanced voltage sags," *Power Syst. Technol.*, vol. 39, no. 3, pp. 601–608, Mar. 2015.
[24] T. Chen, L. Chen, T. Zheng, X. Chen, and S. Mei, "General control strategy to limit peak currents of virtual synchronous generator under voltage sags," in *Proc. IEEE Power Energy Soc. Gen. Meet. (PESGM)*, Boston, MA, USA, Jul. 2016, pp. 1–5.
[25] C. Yaai, L. Jindong, and Z. Jinghua, "Fault ride-through control strategy for solar grid-connected inverters," in *Proc. CSEE*, Jul. 2014, vol. 34. no. 21, pp. 3405–3412.

KAI SHI was born in Suzhou, China, in 1980. He received the B.S. degree in automation and M.S. degree in power electronic and power transmission from Jiangsu University, Zhenjiang, China, in 2002 and 2005, respectively, and the Ph.D. degree in power electronic and power transmission from the Nanjing University of Aeronautics and Astronautics, Nanjing, China, in 2012. Since 2002, he has been with the School of Electrical and Information Engineering, Jiangsu University. Since 2013, he has been an Assistant Professor with Jiangsu University. His current research interests include wind power generator control, grid-connected control, and control strategies of low-voltage ride through.

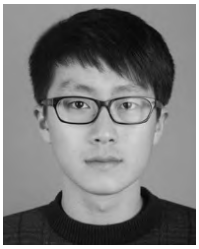

WENTAO SONG was born in Lianyungang, China, in 1995. He received the B.S. degree in electrical engineering from the Jiangsu University of Science and Technology, Zhenjiang, China, in 2017. He is currently a Graduate Student with the School of Electrical and Information Engineering, Jiangsu University, Zhenjiang. His research interests include the novel control strategies of LVRT.

PEIFENG XU was born in Nantong, China, in 1980. She received the B.S. and M.S. degrees in electrical engineering from Jiangsu University, Zhenjiang, China, in 2002 and 2005, respectively. Since 2002, she has been with the School of Electrical and Information Engineering, Jiangsu University. Since 2007, she has been a Lecturer with Jiangsu University. Her current research interests include the design and control of high-efficiency wind power generators.

RONGKE LIU was born in Changzhou, China, in 1977. He received the B.S. degree in mechanical engineering from Southwest Traffic University, Chengdu, China, in 2000. Since 2003, he has been a Senior Engineer with the KTK Group, Changzhou. His main research interests include the mechanical design and integrated design of power supply systems.

ZHIMING FANG was born in Zhenjiang, China, in 1978. He received the M.S. degree in control theory and control engineering from Jiangsu University, Zhenjiang, China, in 2003, and the Ph.D. degree in control theory and control engineering from the Nanjing University of Science and Technology, Nanjing, China, in 2012. Since 2000, he has been a Faculty Member with Jiangsu University, where he is currently a Lecturer. His main research interests include switched systems, nonlinear control, robust control, and parallel robot control.

YI JI was born in Zhenjiang, China, in 1981. He received the B.S. and M.S. degrees from Jiangsu University, Zhenjiang, China, in 2003 and 2006, receptively. Since 2003, he has been with the School of Electrical and Information Engineering, Jiangsu University. Since 2008, he has been a Lecturer with Jiangsu University. His current research interests include signal processing, image processing, and wireless sensor networks application.